Universality and Realistic Extensions to the Semi-Analytic Simulation Principle in GNSS Signal Processing

Ondrej JAKUBOV, Petr KACMARIK, Pavel KOVAR, Frantisek VEJRAZKA

Dept. of Radio Engineering, Czech Technical University in Prague, Faculty of Electrical Engineering, Technická 2, 166 27 Prague 6, Czech republic

jakubon2@fel.cvut.cz, kacmarp@fel.cvut.cz

Abstract. *Semi-analytic simulation principle in GNSS signal processing bypasses the bit-true operations at high sampling frequency. Instead, signals at the output branches of the integrate&dump blocks are successfully modeled, thus making extensive Monte Carlo simulations feasible. Methods for simulations of code and carrier tracking loops with BPSK, BOC signals have been introduced in the literature. Matlab toolboxes were designed and published. In this paper, we further extend the applicability of the approach. Firstly, we describe any GNSS signal as a special instance of linear multi-dimensional modulation. Thereby, we state universal framework for classification of differently modulated signals. Using such description, we derive the semi-analytic models generally. Secondly, we extend the model for realistic scenarios including delay in the feed back, slowly fading multipath effects, finite bandwidth, phase noise, and a combination of these. Finally, a discussion on connection of this semi-analytic model and position-velocity-time estimator is delivered, as well as comparison of theoretical and simulated characteristics, produced by a prototype simulator developed at CTU in Prague.*

Keywords

AltBOC, BPSK, BOC, GNSS, post-correlation modeling, semi-analytic simulation, tracking loops.

1. Introduction

In global navigation satellite systems (GNSS), Monte Carlo simulations became dominant in assessment of algorithm performance. Often, closed-form solutions appear intractable, and explicitly derived formulas need experiments with short implementation time or idealistic conditions. Straightforward generation of high-rate samples and consecutive processing of them is a widely used approach which offers adequate representation of crucial physical phenomena of the communication channel [1], [2].

However, increasing the sampling frequency or algorithm complexity may turn such simulations into a tedious task. This would be the case especially for wideband systems, including all GNSSs. Fortunately, in a large number of systems the most computationally demanding operations can be bypassed with an analytically derived closed-form and statistical description of their outputs, taking the inputs as arguments to their description functions. The rest of the operations are then left untouched. This forms the definition of the *semi-analytic simulation principle* [2].

The problem of semi-analytic modeling in GNSS was first addressed in [3], [4]. The high-rate correlation between the received signal and its replica was avoided by expressing the output as a function of the spreading code autocorrelation function (ACF) and a noise term with known statistical description. The idea turned into a *simulator in the form of Matlab toolbox* [5], [6], named SATLSim. The authors therein developed models for binary-phase-shift-keying (BPSK) and binary-offset-carrier (BOC) modulated signals, processed by code and carrier tracking loops. Evaluation of the tracking jitter, tracking threshold, and mean time to lose lock was discussed.

1.1 Contribution of the Paper

In this paper, we establish a universal framework for description of GNSS modulations. We will see that any of these signals, including the most challenging alternate-binary-offset-carrier (AltBOC), can be expressed as a special case of linear multi-dimensional modulation. Such description would not be further limited if different signals in the inphase and quadrature component were present, including for example composite BOC (CBOC) modulation.

Using such description, we derive the semi-analytic models for the tracking loops. At the expanse generality, the expressions will have the form of vectors and matrices.

In order to adopt this model, which we call as *basic semi-analytic model*, to realistic scenarios, we extend it to account for delay in the feed back, slowly fading multipath, finite bandwidth, phase noise, and combination of these. The model is called as *extended semi-analytic model*.

Not necessarily, these models must be employed only in the investigation of code and carrier tracking loops. Discussion on the connection of these models with multipath mitigation techniques [7] – [11] and position-velocity-time (PVT) estimation [12], [7] is provided. Investigation of various advanced algorithms such as vector tracking [13] – [18], direct positioning [19], [20] turns out to be possible using the semi-analytic approach, as well.

Finally, a Matlab-based toolbox using object-oriented programming with its graphical user interface (GUI) has been developed at CTU in Prague. It provides simulation characteristics of feed-back systems for civil GPS, Galileo, and GLONASS signals. It is freely downloadable at [21].

1.2 Notation

All vectors in the text are column vectors, denoted with bold emphasize, as matrices are. The operators $\mathrm{Av}[.]$, $\mathrm{E}[.]$ denote time average and expectation, respectively. We use symbol $\mathcal{R}_{(.)}(.)$ to represent correlation functions in continuous time, symbol $\mathcal{R}_{(.)}[.]$ for correlation functions in discrete time. Symbol $\mathcal{S}_{(.)}(.)$ denotes power spectral density (PSD). Symbol $\mathcal{F}[.]$ is the Fourier transform operator. From the context, it will always be clear what exactly each operator refers to. Symbol $\delta(.)$ denotes Dirac delta function, symbol $\delta[.]$ the unit impulse. Symbol $[.]_{i,j}$ denotes an element with indices i, j. Symbol $\sum_n$ denotes the summation over index n with unspecified lower and upper bounds, extending over an infinitive range. We use a notation $\mathrm{Trig}_T(\tau)$ for the following triangular function

$$\mathrm{Trig}_T(\tau) = \begin{cases} 1 - \frac{|\tau|}{T}, & |\tau| < T, \\ 0, & \text{else} \end{cases} \tag{1}$$

and notation $\mathrm{Rect}_T(\tau)$ for the following rectangular function

$$\mathrm{Rect}_T(\tau) = \begin{cases} 1, & 0 \leq \tau < T, \\ 0, & \text{else.} \end{cases} \tag{2}$$

2. GNSS Signals as Linear Multi-Dimensional Modulations

In this section, we define the linear multi-dimensional modulation (LMDM) and represent BPSK(γ), BOC(β,γ), AltBOC(15,10) modulations in that manner. We also show, how signals with inphase and quadrature components representing different signals can be expressed as a kind of such modulation. The TMBOC modulation of GPS L2C signal is not discussed separately, but neglecting the property of the long period of the L2 CL-code, our model can still be applied. This simplification would make no difference since the LMDM representation is developed for the simulation where code acquisition is a priori assumed to be done.

2.1 Linear Multi-Dimensional Modulation

The modulated signal $s(t)$ at time t is assumed to be an additive composition of vector modulation impulses $\mathbf{h}(t)$ multiplied by vector of channel symbols $\mathbf{q}_n^T$ generated at discrete time n, corresponding to n multiples of the channel symbol period T_s in continuous time, [22]

$$s(t) = \sum_n \mathbf{q}_n^T \mathbf{h}(t - nT_s). \tag{3}$$

We denote the dimension of the modulation impulse vector and the channel symbol vector as $N_h = \dim \mathbf{h}(t) = \dim \mathbf{q}_n$. The channel symbols $\mathbf{q}_n$ are a function of the data symbols $\mathbf{d}_n$ and the inner states of the discrete part of the modulator. We suppose that the channel symbols are equiprobable, independent and identically distributed (EP-IID), $\mathrm{E}\left[\mathbf{q}_{n+m}\mathbf{q}_n^T\right] = \delta[m]\,\mathbf{I}$, and that the diagonal elements of the correlation matrix $\boldsymbol{\mathcal{R}}_{\mathbf{h}}(\tau)$ of the modulation impulse

$$\boldsymbol{\mathcal{R}}_{\mathbf{h}}(\tau) = \int_{-\infty}^{\infty} \mathbf{h}(t+\tau)\mathbf{h}^H(t)\mathrm{d}t \tag{4}$$

have unit energy $\forall i \in \{1, \dots N_h\}: \left|[\boldsymbol{\mathcal{R}}_{\mathbf{h}}(0)]_{i,i}\right| = 1$.

2.2 BPSK(γ)

According to [7], the BPSK(γ) modulated signal can be defined as a BPSK direct-sequence-spread-spectrum (DS-SS) signal with chip length $T_c = T_0/\gamma$ where $T_0 = 1/1023$ ms, $\gamma \in \mathbb{N}$

$$s_{\mathrm{BPSK}(\gamma)}(t) = \sum_n q_n h(t - nT_s). \tag{5}$$

In (5), it holds that $q_n \in \{-1, 1\}$, $N_h = 1$, and the modulation impulse contains the whole number of code periods $N_s = T_s/(N_c T_c) \in \mathbb{N}$ per a channel symbol. Symbol N_c denotes the number of chips in a code period. The modulation impulse is depicted in Fig. 1 (left). The autocorrelation function of the modulation impulse can be approximated as a triangular function in Fig. 1 (right), $\mathcal{R}_{h,\mathrm{BPSK}(\gamma)}(\tau) \approx \mathrm{Trig}_{T_c}(\tau)$, for details see [7].

2.3 BOC(β,γ)

The BOC(β,γ) modulated signal is a BPSK(γ) modulated signal multiplied by an alternating periodic signal [23], named *subcarrier*,

$$\sum_i (-1)^i \mathrm{Rect}_{T_r}(t - iT_r) \tag{6}$$

with period $2T_r$ such that $\beta = T_0/(2T_r)$. We define N_r as the number of multiplying rectangles on one chip, then $N_r = 2\beta/\gamma$. The leading edge of the subcarrier is always coincident with the leading edge of a chip. An illustrative example of BOC(1,1) modulated signal (Galileo E1b or E1c) is given in Fig. 2. It holds that $q_n \in \{-1, 1\}$, $N_h = 1$, and the modulation impulse equals BPSK(γ) modulation impulse (Fig. 1 left) multiplied by the alternating signal in (6). The autocorrelation function of the modulation impulse $\mathcal{R}_h(\tau)$ can be derived using similar approach as in [23]

$$\mathcal{R}_h(\tau) = \frac{1}{N_r} \sum_{i=0}^{N_r-1} \sum_{i'=0}^{N_r-1} (-1)^{i-i'} \mathrm{Trig}_{T_r}\left(\tau - \left(i - i'\right) T_r\right). \tag{7}$$

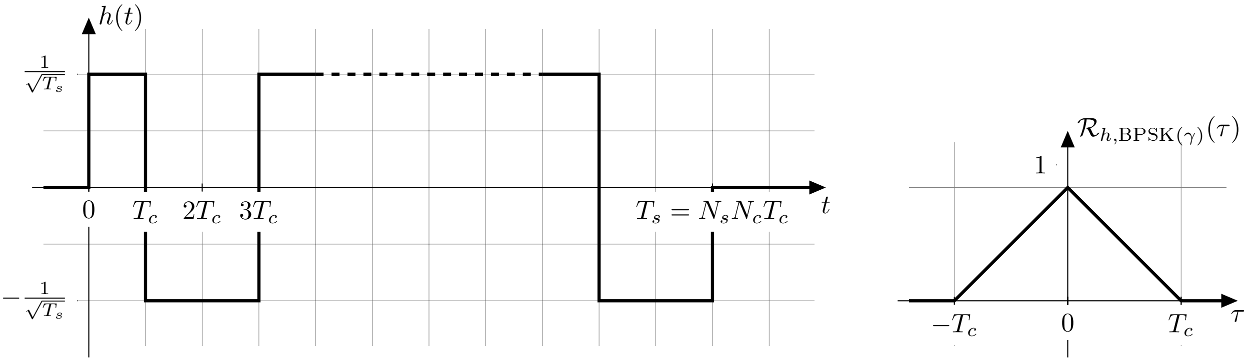

Fig. 1. Modulation impulse $h(t)$ of BPSK(γ) modulation (left), approximated ACF of the modulation impulse $\mathcal{R}_h(\tau)$ (right).

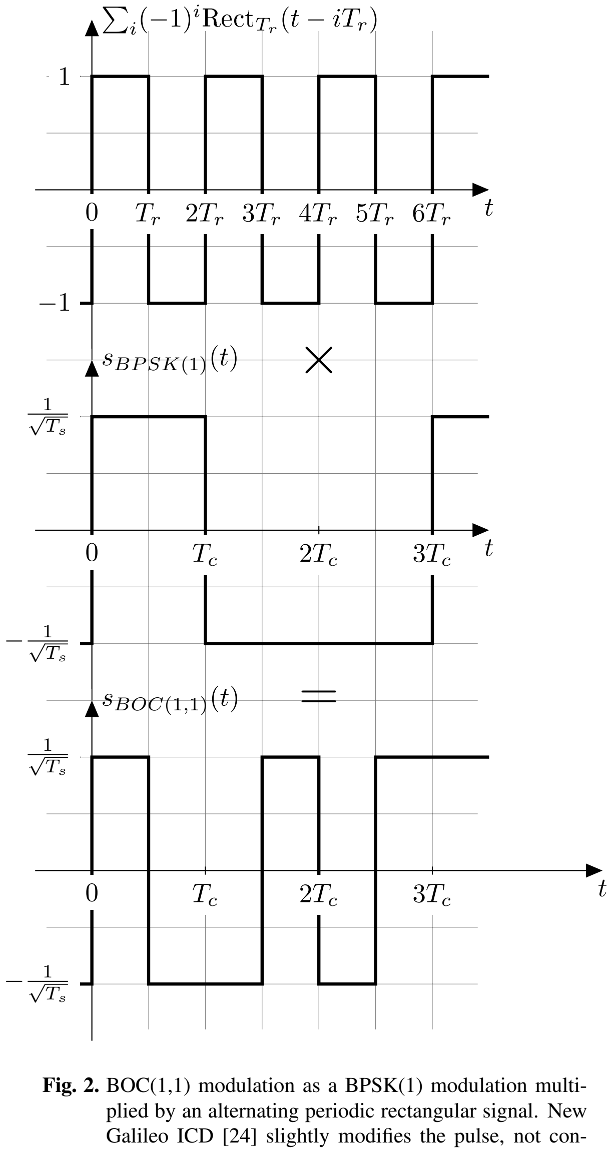

Fig. 2. BOC(1,1) modulation as a BPSK(1) modulation multiplied by an alternating periodic rectangular signal. New Galileo ICD [24] slightly modifies the pulse, not constraining the approach used here.

In our BOC(1,1) example, $N_r = 2$, $T_r = T_0/2$, hence

$$\mathcal{R}_{h,\mathrm{BOC}(1,1)}(\tau) = \frac{1}{2}\left(2\mathrm{Trig}_{T_r}(\tau) - \mathrm{Trig}_{T_r}(\tau - T_r) - \mathrm{Trig}_{T_r}(\tau + T_r)\right).$$

The autocorrelation function $\mathcal{R}_{h,\mathrm{BOC}(1,1)}(\tau)$ is depicted in Fig. 3.

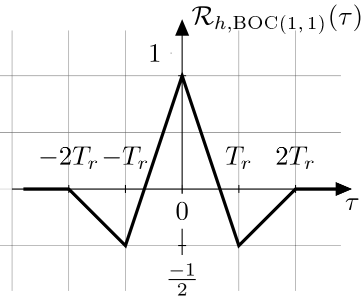

Fig. 3. ACF of BOC(1,1) modulation impulse.

2.4 The IQ Extension of BPSK(γ), BOC(β,γ)

In some cases, modulated signals are transmitted in the inphase and quadrature components at the same time. Provided the channel symbols are generated with the same period T_s, the modulated signal can be expressed as

$$\begin{aligned} s(t) &= \sum_n q_{n,I} h_I(t - nT_s) + \mathrm{j}\sum_n q_{n,Q} h_Q(t - nT_s) \\ &= \sum_n \mathbf{q}_n^T \mathbf{h}(t - nT_s) \end{aligned}$$

where $N_h = 2$, $\mathbf{q}_n = [q_{n,I}\ \mathrm{j}q_{n,Q}]^T$, $\mathbf{h}(t) = [h_I(t)\ h_Q(t)]^T$. The correlation matrix follows

$$\boldsymbol{\mathcal{R}}_{\mathbf{h}}(\tau) \approx \begin{pmatrix} \mathcal{R}_{h_I}(\tau) & 0 \\ 0 & \mathcal{R}_{h_Q}(\tau) \end{pmatrix}. \quad (8)$$

Frequently, the quadrature component has the form of pilot signal and no data are present, then $q_{n,Q} = 1$. An example may be the Galileo E1b, E1c signals.

2.5 AltBOC(15,10)

The AltBOC(15,10) modulation, explicitly defined in [24], is a nonlinear modulation

$$s_{\mathrm{AltBOC}(15,10)}(t) = \sum_n h(\mathbf{q}_n, t - nT_s) \quad (9)$$

where $\mathbf{q}_n = [q_{n,1}\, q_{n,2}]^T$, $q_{n,1}, q_{n,2} \in \{-1, 1\}$. Symbol $h(\mathbf{q}_n, t)$ denotes the modulation function essentially nonzero on $\langle 0, T_s)$. Here, we assume T_s to be 1 ms = duration of one code period. Nevertheless, this approach will enable us to easily represent the AltBOC(15,10) signal as an LMDM. We define the following couple of channel symbol vector $\mathbf{q}'_n$ and modulation impulse vector $\mathbf{h}'(t)$ such that

$$\mathbf{q}'_n = \begin{cases} [1\,0\,0\,0]^T & \text{for } \mathbf{q}_n = \mathbf{q}_n^{\{1\}}, \\ [0\,1\,0\,0]^T & \text{for } \mathbf{q}_n = \mathbf{q}_n^{\{2\}}, \\ [0\,0\,1\,0]^T & \text{for } \mathbf{q}_n = \mathbf{q}_n^{\{3\}}, \\ [0\,0\,0\,1]^T & \text{for } \mathbf{q}_n = \mathbf{q}_n^{\{4\}}, \end{cases} \tag{10}$$

$$\mathbf{h}'(t) = \begin{bmatrix} h(\mathbf{q}_n^{\{1\}}, t) \\ h(\mathbf{q}_n^{\{2\}}, t) \\ h(\mathbf{q}_n^{\{3\}}, t) \\ h(\mathbf{q}_n^{\{4\}}, t) \end{bmatrix} \tag{11}$$

where $\mathbf{q}_n^{\{1\}} = [-1\,-1]^T$, $\mathbf{q}_n^{\{2\}} = [-1\,1]^T$, $\mathbf{q}_n^{\{3\}} = [1\,-1]^T$, $\mathbf{q}_n^{\{4\}} = [1\,1]^T$. The AltBOC(15,10) can then be rewritten as an LMDM without the EP-IID property of channel symbols

$$s_{\text{AltBOC}(15,10)}(t) = \sum_n \mathbf{q}_n'^T \mathbf{h}'(t - nT_s). \tag{12}$$

The correlation matrix $\mathcal{R}_{\mathbf{h}'}(\tau)$ of the modulation impulse is then, using results from [25],

$$\mathcal{R}_{\mathbf{h}'}(\tau) = \begin{pmatrix} \mathcal{R}_{h,00}(\tau) & \mathcal{R}_{h,01}(\tau) & \mathcal{R}_{h,10}(\tau) & \mathcal{R}_{h,11}(\tau) \\ \mathcal{R}_{h,01}(\tau) & \mathcal{R}_{h,00}(\tau) & \mathcal{R}_{h,11}(\tau) & \mathcal{R}_{h,10}(\tau) \\ \mathcal{R}_{h,10}(\tau) & \mathcal{R}_{h,11}(\tau) & \mathcal{R}_{h,00}(\tau) & \mathcal{R}_{h,01}(\tau) \\ \mathcal{R}_{h,11}(\tau) & \mathcal{R}_{h,10}(\tau) & \mathcal{R}_{h,01}(\tau) & \mathcal{R}_{h,00}(\tau) \end{pmatrix} \tag{13}$$

where correlation functions $\mathcal{R}_{h,00}$, $\mathcal{R}_{h,01}$, $\mathcal{R}_{h,10}$, $\mathcal{R}_{h,11}$ are depicted in Fig. 4.

3. Basic Model: Semi-Analytic Approach

In this section, we derive the basic model of the post-correlator signals for LMDM. We suppose the *linear additive white Gaussian noise* (AWGN) channel with *slowly time varying parameters* (STVP) [26], [27]. This model is here named as *basic*.

3.1 Channel Model

Linear AWGN channel models the received signal $x(t)$ as the transmitted signal with data symbols $\mathbf{d} = [\ldots \mathbf{d}_n \ldots]^T$ shifted in time by delay $\tau_0 > 0$, multiplied by a carrier with time varying phase $\varphi(t) = 2\pi f_s t + \varphi_0$ where $\varphi_0 \in \mathbb{R}$ is the carrier phase offset and $f_s \in \mathbb{R}$ is the frequency shift. Such signal is then attenuated in the channel by $\alpha_0 > 0$ and is embedded in complex WGN $w(t) \in \mathbb{C}$ with double-sided power spectral density $2N_0$, $N_0 > 0$

$$x(t) = \alpha_0 \exp(\mathrm{j}\varphi(t))\, s(t - \tau_0, \mathbf{d}) + w(t). \tag{14}$$

The parameters τ_0, φ_0, f_s, α_0, N_0 are said to be slowly time varying with respect to T_s. We also make the assumption that $f_s T_s < \pi$. This condition holds after a successful acquisition.

3.2 Representation of Correlator Output Signals

Let $\mathcal{Z}(\Delta\tau_s)$ denote the vector of correlator output signals at time nT_s in the following form

$$\mathcal{Z}(\Delta\tau_s) = \int_{-\infty}^{\infty} x(t) \exp\left(-\mathrm{j}\hat{\varphi}(t, \hat{f}_s)\right) \mathbf{h}^*\left(t - nT_s - \hat{\tau}_0 + \Delta\tau_s\right) \mathrm{d}t \tag{15}$$

where $\hat{\varphi}(t)$ is the estimate of the carrier phase at time t depending on carrier frequency estimate $\hat{f}_s$. Symbol $\hat{\tau}_0$ is the estimate of the signal delay, and $\Delta\tau_s$ is the time shift of the replicated modulation impulse. The situation is depicted in Fig. 5.

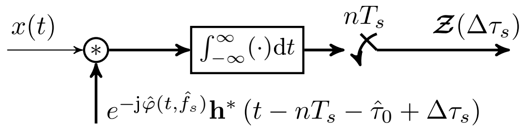

Fig. 5. Correlator output signals and their calculation. Bold lines represent vectors.

Substituting (3) into (14) and the result into (15), we see that $\mathcal{Z}(\Delta\tau_s)$ can be decomposed into the useful component $\mathcal{X}(\Delta\tau_s)$ and the noise component $\mathcal{N}(\Delta\tau_s)$

$$\mathcal{Z}(\Delta\tau_s) = \mathcal{X}(\Delta\tau_s) + \mathcal{N}(\Delta\tau_s) \tag{16}$$

where

$$\begin{aligned} \mathcal{X}(\Delta\tau_s) &= \alpha_0 \exp\left(\mathrm{j}(\varphi - \hat{\varphi})\right) \qquad (17) \\ &\quad \cdot \operatorname{sinc}\left(\left(f_s - \hat{f}_s\right) T_s\right) \mathcal{R}_{\mathbf{h}}^T\left(\tau_0 - \hat{\tau}_0 - \Delta\tau_S\right) \mathbf{q}_n \end{aligned}$$

where $\varphi = 2\pi f_s n T_s + \varphi_0$ and $\hat{\varphi} = \hat{\varphi}(nT_s)$. The noise component $\mathcal{N}(\Delta\tau_s)$ can be modeled as zero mean white Gaussian noise vector uncorrelated over time n, but correlated over elements with the following covariance matrix $\mathbf{C}_{\mathcal{N}(\Delta\tau_s)} = 2N_0 \mathcal{R}_{\mathbf{h}}(0)$. However, $\mathcal{Z}(\Delta\tau_s)$ signals for various values of $\Delta\tau_s$ are evaluated in practice and the vectors $\mathcal{N}(\Delta\tau_s)$ then become correlated over each other. This would be the case for early/late components $\mathcal{Z}_E = \mathcal{Z}(-\Delta\tau)$, $\mathcal{Z}_L = \mathcal{Z}(\Delta\tau)$, $0 < \Delta\tau < T_c$, where $2\Delta\tau$ is sometimes referred as correlator spacing. If $\mathcal{N}$ concatenates the early/late noise components $\mathcal{N} = \left[\mathcal{N}_E^T\, \mathcal{N}_L^T\right]^T$ where $\mathcal{N}_E = \mathcal{N}(-\Delta\tau)$, $\mathcal{N}_L = \mathcal{N}(\Delta\tau)$, the vector $\mathcal{N}$ is also a zero mean WGN vector with the following covariance matrix

$$\mathbf{C}_{\mathcal{N}} = 2N_0 \begin{pmatrix} \mathcal{R}_{\mathbf{h}}(0) & \mathcal{R}_{\mathbf{h}}(2\Delta\tau) \\ \mathcal{R}_{\mathbf{h}}(-2\Delta\tau) & \mathcal{R}_{\mathbf{h}}(0) \end{pmatrix}. \tag{18}$$

The concatenated noise component $\mathcal{N}$ can be generated as

$$\mathcal{N} = \mathbf{A}\boldsymbol{\eta} \tag{19}$$

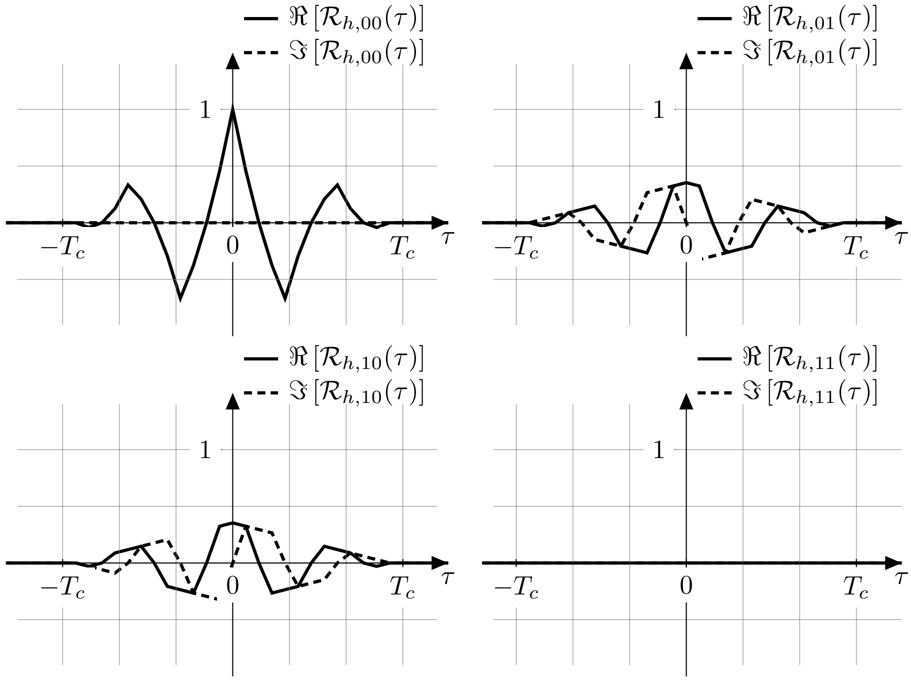

Fig. 4. Correlation functions $\mathcal{R}_{h,00}$, $\mathcal{R}_{h,01}$, $\mathcal{R}_{h,10}$, $\mathcal{R}_{h,11}$ of the correlation matrix $\boldsymbol{\mathcal{R}}_{\mathbf{h}'}(\tau)$ for LMDM representation of AltBOC(15,10) modulation.

where $\boldsymbol{\eta} \sim \mathcal{N}(\mathbf{0}, \mathbf{I})$ and $\mathbf{C}_{\mathcal{N}} = \mathbf{A}\mathbf{A}^H$. Matrix $\mathbf{A}$ can be obtained using Choleski decomposition. Vector $\boldsymbol{\eta}$ can be easily generated in Matlab or any similiar software. The group delay introduced by the integration in (15) is discussed in Section 4.

Strictly speaking, the convenience of post-correlator modeling is due to the fact that the output signals $\mathcal{Z}(\Delta\tau_s)$ become sufficient statistics for the maximum likelihood (ML) estimation of $\tau_0, \varphi_0, f_s, \alpha_0, N_0, \mathbf{d}$, under the above mentioned conditions [26], [27], [28]. Hence, the semi-analytic models of the tracking loops in [5], [6] may have been developed. In this paper, we do not embody the post-correlator model into a particular structure, instead, we develop a general model which can be adopted to an arbitrary system fulfilling the assumptions.

We inherently supposed that the integration time was chosen as channel symbol period T_s. If shorter integration times are desired in the simulation, the modulation impulse vector $\mathbf{h}(t)$ may account for smaller number of code periods or only one. The channel symbols then lose the stationarity and EP-IID property. We will see that this fact does not prevent us from using the developed models, except for the bandwidth constriction which is out of scope of this paper.

3.3 Summary

In order to sum up this section, we recall that a correlator output signal expressed as an LMDM in linear AWGN channel with STVP can be modeled as depicted in Fig. 6. In that figure, output signals for $\Delta\tau_s = \Delta\tau_1, \ldots, \Delta\tau_K$ are generated $\forall k \in \{1, \ldots, K\} : 0 < \Delta\tau_k < T_c$

$$\mathcal{Z} = \begin{bmatrix} \mathcal{Z}(\Delta\tau_1) \\ \vdots \\ \mathcal{Z}(\Delta\tau_K) \end{bmatrix},$$

$$\mathcal{X} = \begin{bmatrix} \mathcal{X}(\Delta\tau_1) \\ \vdots \\ \mathcal{X}(\Delta\tau_K) \end{bmatrix}, \mathcal{N} = \begin{bmatrix} \mathcal{N}(\Delta\tau_1) \\ \vdots \\ \mathcal{N}(\Delta\tau_K) \end{bmatrix}$$

where the correlation matrix of the concatenated noise component is

$$\mathbf{C}_{\mathcal{N}} = 2N_0 \begin{pmatrix} \boldsymbol{\mathcal{R}}_{\mathbf{h}}(0) & \cdots & \boldsymbol{\mathcal{R}}_{\mathbf{h}}(\Delta\tau_K - \Delta\tau_1) \\ \vdots & \ddots & \vdots \\ \boldsymbol{\mathcal{R}}_{\mathbf{h}}(\Delta\tau_1 - \Delta\tau_K) & \cdots & \boldsymbol{\mathcal{R}}_{\mathbf{h}}(0) \end{pmatrix}.$$

4. Extended Model: Realistic Phenomena

In this section, we extend our model to a more realistic situation. Firstly, we show how feed-back delay may be embodied in the model. Secondly, we consider slowly fading multipath channel with AWGN. We will see that the tapped-delay-line model (TDLM) of the received signal will, thanks to the linearity of correlation, simply result in an additive composition of the separate delay-line components. Thirdly, we discover that bandwidth constriction of the received sig-

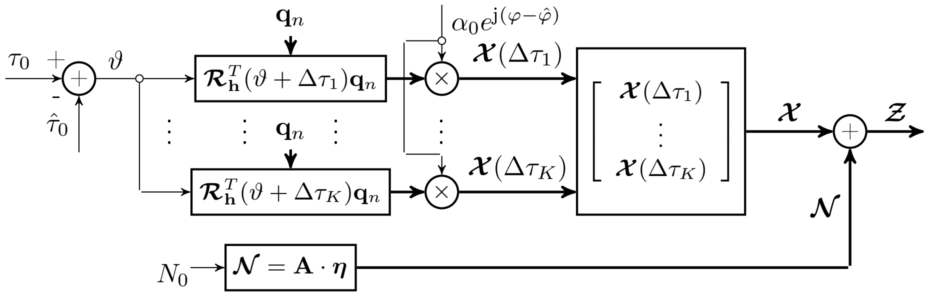

Fig. 6. Basic model of the correlator output signals generated as LMDM in linear AWGN channel with STVP. Bold lines represent vectors.

nal will result in bandwidth constriction of the correlation matrix. The modified correlation matrix would then be possible to store to memory and reload its values when generation of the output signals. Fourthly, we will discuss how phase noise with $1/f^2$ phase noise characteristics may be added to the true parameters. Finally, a combination of these phenomena is turned into a complex scheme.

4.1 Multipath

Let us suppose that the received signal is composed of $L+1$ line-of-sight components with amplitude $\alpha_l > 0$, carrier phase offset $\varphi_l \in \mathbb{R}$, and code delay $\tau_l > 0$

$$x(t) = \sum_{l=0}^{L} \alpha_l \exp\left(\mathrm{j}\left(2\pi f_s t + \varphi_l\right)\right) s(t-\tau_l, \mathbf{d}) + w(t). \quad (20)$$

The output signals of the correlators $\boldsymbol{\mathcal{Z}}(\Delta\tau_s)$ can be expressed by first substituting (3) to (20), the result then into (15). We get that

$$\boldsymbol{\mathcal{Z}}(\Delta\tau_s) = \sum_{l=0}^{L} \boldsymbol{\mathcal{X}}_l(\Delta\tau_s) + \boldsymbol{\mathcal{N}}(\Delta\tau_s)$$

with lth useful signal component

$$\begin{aligned} \boldsymbol{\mathcal{X}}_l(\Delta\tau_s) &= \alpha_l \exp\left(\mathrm{j}\left(\phi_l - \hat{\phi}_0\right)\right) \operatorname{sinc}\left(\left(f_s - \hat{f}_s\right) T_s\right) \\ &\quad \cdot \boldsymbol{\mathcal{R}}_{\mathbf{h}}^T\left(\tau_l - \hat{\tau}_0 + \Delta\tau_s\right) \mathbf{q}_n. \end{aligned}$$

We use notation ϕ_l for the actual carrier phase of the lth component at time nT_s, then it holds that $\phi_l = 2\pi f_s n T_s + \varphi_l$.

4.2 Finite Bandwidth

In this subsection, we will derive the power spectral density of a GNSS signal as an LMDM. We consider that channel symbols are EP-IID. This assumption does not hold for our IQ representation where one of the channel symbol is constant. We will discuss this case separately.

The power spectral density (PSD) $\mathcal{S}_s(f)$ of a modulated signal $s(t)$ equals, according to the Wiener-Khinchin theorem,

$$\mathcal{S}_s(f) = \mathcal{F}\left[\mathcal{R}_s(\tau)\right]$$

where

$$\mathcal{R}_s(\tau) = \mathrm{AvE}\left[s(t+\tau)s^*(t)\right].$$

For all linear multidimensional modulations with stationary channel symbols, it holds that [22]

$$\mathcal{S}_s(f) = \frac{1}{T_s}\mathbf{H}^H(f)\boldsymbol{\mathcal{S}}_{\mathbf{q}}(fT_s)\mathbf{H}(f) \quad (21)$$

where

$$\begin{aligned} \mathbf{H}(f) &= \mathcal{F}\left[\mathbf{h}(t)\right] \\ &= \left[\mathcal{F}\left[h_1(t)\right] \mathcal{F}\left[h_2(t)\right] \ldots \mathcal{F}\left[h_{N_h}(t)\right]\right]^T, \\ \boldsymbol{\mathcal{S}}_{\mathbf{q}}(F) &= \sum_{m=-\infty}^{\infty} \boldsymbol{\mathcal{R}}_{\mathbf{q}}[m] e^{-\mathrm{j}2\pi F m}, \\ \boldsymbol{\mathcal{R}}_{\mathbf{q}}[m] &= \mathrm{E}\left[\mathbf{q}_{n+m}\mathbf{q}_n^H\right]. \end{aligned}$$

With EP-IID and zero mean channel symbols, we have

$$\boldsymbol{\mathcal{R}}_{\mathbf{q}}[m] = \delta[m] \operatorname{diag}\left(\mathrm{E}\left[\left|q_{0,1}\right|^2\right], \ldots, \mathrm{E}\left[\left|q_{0,N_h}\right|^2\right]\right)$$

for all our modulations $\mathrm{E}\left[\left|q_{0,k}\right|^2\right] = c$, $c > 0$ for all $k \in \{1, \ldots, N_h\}$, thus

$$\begin{aligned} \boldsymbol{\mathcal{R}}_{\mathbf{q}}[m] &= c\mathbf{I}\delta[m], \\ \boldsymbol{\mathcal{S}}_{\mathbf{q}}(F) &= c\mathbf{I} \end{aligned}$$

and finally

$$\mathcal{S}_s(f) = \frac{c}{T_s}\mathbf{H}^H(f)\mathbf{H}(f).$$

Let $\mathbf{S}_{\mathrm{FBW}}(f)$ be the PSD of signal $s(t)$ constrained with an ideal low-pass filter of $BW/2$ band-stop frequency

$$\mathbf{S}_{\mathrm{FBW}}(f) = \begin{cases} \mathbf{S}(f), & |f| < BW/2, \\ \mathbf{0}, & \text{else.} \end{cases}$$

The constrained PSD of the signal

$$\mathcal{S}_{s,\mathrm{FBW}}(f) = \frac{c}{T_s}\mathbf{H}_{\mathrm{FBW}}^H(f)\mathbf{H}_{\mathrm{FBW}}(f)$$

will constrain the Fourier transform of the modulation impulse vector

$$\mathbf{H}_{\mathrm{FBW}}(f) = \begin{cases} \mathbf{H}(f), & |f| < BW/2, \\ \mathbf{0}, & \text{else.} \end{cases}$$

The truncation of the spectrum of the modulation impulses can then be accomplished in Matlab by the following steps:

1. Calculate the Fourier transform of the modulation impulse correlation matrix

$$\boldsymbol{\rho}_{\mathbf{h}}(f) = \mathcal{F}\left[\boldsymbol{\mathcal{R}}_{\mathbf{h}}(\tau)\right],$$

2. truncate it in frequency domain

$$\boldsymbol{\rho}_{\mathbf{h},\mathrm{FBW}}(f) = \begin{cases} \boldsymbol{\rho}_{\mathbf{h}}(f), & |f| < BW/2, \\ 0, & \text{else} \end{cases}$$

3. and calculate inverse Fourier transform

$$\boldsymbol{\mathcal{R}}_{\mathbf{h},\mathrm{FBW}}(\tau) = \mathcal{F}^{-1}\left[\boldsymbol{\rho}_{\mathbf{h},\mathrm{FBW}}(f)\right].$$

Considering the IQ extension of BPSK(γ) or BOC(β,γ) modulations, the channel symbol vector would not be generally EP-IID, since $q_{n,Q} = 1$. It results in the fact that $\boldsymbol{\mathcal{S}}_{\mathbf{q}}(fT_s) \neq c\mathbf{I}$ in (21). Nevertheless, we bypass the problem by supposing that bandwidth constriction will not influence the flow of transmitted channel symbols, but the modulation impulse vector. It substantiates us to use the procedures 1-3 to constrain the received signal.

The transformations are here represented in continuous time domain. However, computationally more attractive would be to accomplish the constriction in discrete time domain using the fast Fourier transform (FFT), and store the samples of the constrained correlation matrix in memory. On load, an interpolation may be employed to better approximate the continuous function.

4.3 Phase Noise

The carrier phase noise signal can be modeled as zero mean Gaussian additive component φ_{PN} to the carrier phase, with defined *phase noise characteristics* $\mathcal{L}_\varphi(f)$ – normalized single-sided power spectral density of φ_{PN}. The same definition stands for the code phase noise signal τ_{PN}, being additive to the code delay. Its influence is not significant relative to φ_{PN}. We model the phase noise characteristics $\mathcal{L}_\varphi(f)$ with the following function

$$\mathcal{L}_\varphi(f) = \begin{cases} \sigma^2, & |f| < f_0, \\ a^2\sigma^2/f^2, & \text{else,} \end{cases}$$

depicted in Fig. 7. Signals φ_{PN}, τ_{PN} can be obtained by generating white Gaussian noise with variance σ^2, and passing it through linear time-invariant (LTI) system with frequency response $\mathcal{G}(f)$ such that ($a > 0$)

$$|\mathcal{G}(f)| = \begin{cases} 1, & |f| < f_0, \\ a/f, & \text{else.} \end{cases}$$

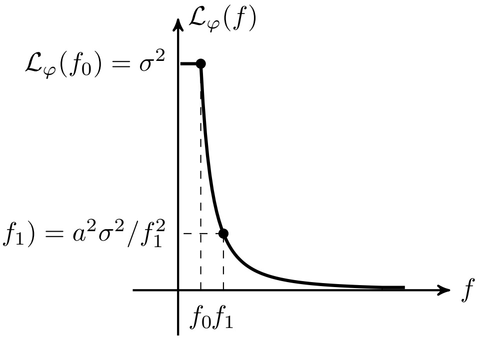

Fig. 7. Model of the carrier phase noise characteristics $\mathcal{L}_\varphi(f)$.

4.4 Feed-Back Delay

Since the integration in (15) can be classified as a signal propagation through a linear time-invariant (LTI) system with $\mathrm{Rect}_{T_s}(t + nT_s)$ impulse response, group delay $T_s/2$ is introduced by that operation. In discrete time with sampling period T_s, this can be modeled with the moving average

$$\frac{1}{2}\left(\mathcal{Z}_n(\Delta\tau_s) + \mathcal{Z}_{n-1}(\Delta\tau_s)\right) \qquad (22)$$

where index n is used to denote the time in multiples of integration time T_s.

Additionally, we can model an integer delay in the feed-back, denoted as D_τ, D_φ for code and carrier phase, respectively, simply by adding FIFO memory. Then, we store the samples and read them back using a circular buffer, in order to reduce the computational complexity.

4.5 Combined Model

We can connect the above mentioned models in order to get the *extended model* in Fig. 8. Due to linearity of the TDLM, the finite bandwidth would clearly constrain each correlation matrix. Extension of the phase noise model and feed-back delay model is straightforward.

5. Complex System Model: PVT Estimation

In [5], [6], the semi-analytic models were applied to investigate behavior of the code and carrier tracking loops. However, the approach might be incorporated to simulations of much more complex systems. As an example, based on the satellite constellation and true user PVT, input parameters to the basic model (τ, f_s, φ, α, N_0) can be generated, then they can propagate through the model, and the output values can be further processed. By further processing we mean for instance PVT estimation. Optionally, feed-back between the PVT estimator and the model may be established in order to simulate vector tracking or direct positioning algorithms.

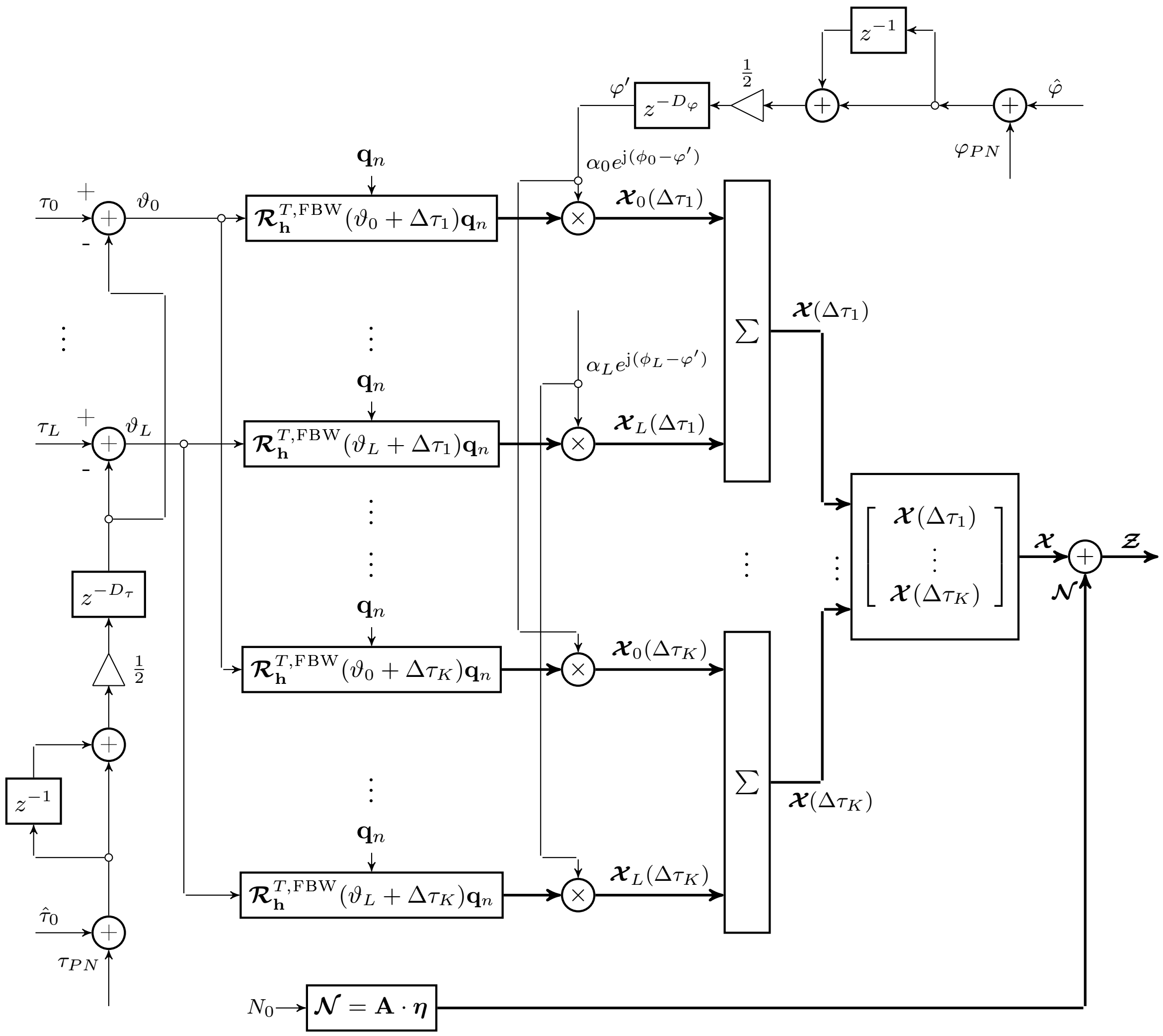

Fig. 8. Extended model of the correlator output signals generated as LMDM in slowly fading TDLM in AWGN channel with FBW, feed-back delay, and phase noise. Bold lines represent vectors.

Section 4 also provides hints how the model can be incorporated in simulations of multipath mitigation techniques which supposes a slowly fading channel. Slight modifications of the model would suffice most of the proposed methods adopting correlation [8] – [11], [13] – [20], [30], [31].

6. Developed Simulator

A simulator of GNSS tracking loops, using the extended model as an underlying block, has been developed at CTU in Prague. Its name is *GNSSTracker*. The simulator was designed in the Matlab environment with the object-oriented programming approach. It has an encapsulating graphical user interface (GUI). A quick tutorial to the simulator is available in [29], the simulator itself at [21].

A GNSS signal may be represented as LMDM in class `Setup` by definition of the correlation matrix $\boldsymbol{\mathcal{R}}_{\mathbf{h}}(\tau)$, the channel symbol vector $\mathbf{q}_n$, and some other constants concerning the modulated signal. Class `CorrOut` represents the extended model itself. The multipath channel is here restricted to a 2-path channel.

Classes `DLL`, `PLL` represent a delay-locked loop and a phase-locked loop, respectively, and define the properties of the discriminator and loop filter. Both `DLL`, `PLL` are subclasses of abstract class `FBS` (feed-back system). Classes `Motion`, `Sources`, `Signals` provide the FBSs with the input parameters changing over time as requested by class `Tracking`, which is responsible for the loops' closure. The input signals might be step, ramp, frequency ramp, or signal simulating the mutual motion between the user and the space vehicle (SV).

Based on the Monte Carlo simulation principle, characteristics of the equivalent model, multipath, mean square error (MSE), and synchronization failure can be estimated. It is ensured by classes `Eq_model`, `Multipath`, `MSE`, `SyncFail`, respectively. Transient responses can be visualized, as well, with methods of the class `Tracking`. Hierarchy of the classes is depicted in Fig. 9.

7. Simulation Results

The correctness of the model and the functionality of the simulator have been verified in the following manner. Well known characteristics were simulated and compared with their theoretical values. Characteristics known from bit-true simulations were compared with the simulated ones in *GNSSTracker*. To be more specific, discriminator characteristics, tracking jitters, multipath characteristics of BPSK(1), BOC(1,1), AltBOC(15,10) modulated signals in various system setups were consulted with [7], [23], [25], [30].

In this paper, we present simulation results of AltBOC(15,10) fully optimal processing introduced in [31]. The method employs four complex early/late correlators ($N_h = 4$, $\dim(\boldsymbol{\mathcal{Z}}) = 8$) and can be classified as joint-maximum-likelihood estimation of the signal parameters and channel symbols [26], [27]. Each of the four correlators calculates a metric for decision about the pair of actual channel symbols. The output of the selected branch is then fed to the DLL and PLL discriminators.

In the simulation, we consider the extended model from Fig. 8. The setup of the simulation is in Tab. 1. In Fig. 10, the characteristics of discriminator, loop noise variance, multipath, and mean square error are presented.

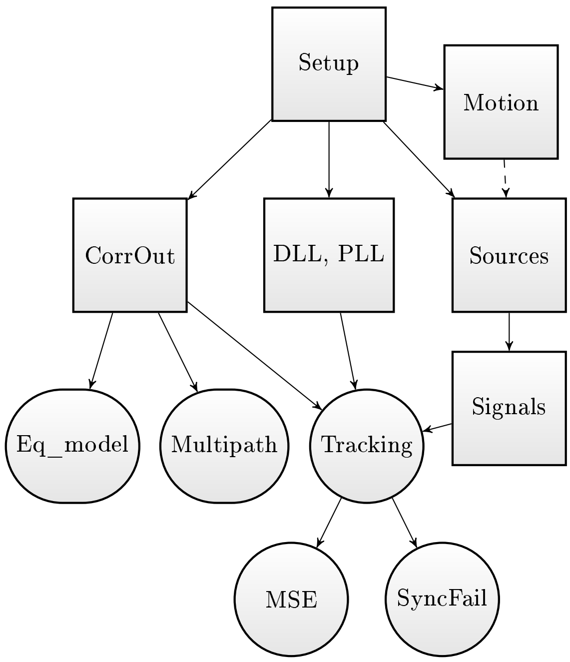

Fig. 9. Class hierarchy in GNSS tracking toolbox (*GNSSTracker*). Classes with the shape of rounded rectangle are intended for simulations. The dashed line denotes an input which is optional.

It is apparent from the figure that the discriminator characteristics of the DLL has multiple stable lock points which is a consequence of the alternating shape of the correlation function $\Re[\mathcal{R}_{b,00}(\tau)]$ in Fig. 4. The narrow peak of $\Re[\mathcal{R}_{b,00}(\tau)]$ at $\tau = 0$ and narrow correlator spacing $\Delta\tau$ result in a steep zero crossing of the characteristics. The peaks are rounded due to the finite bandwidth. PLL discriminator characteristics is linear over $\langle -\pi, \pi \rangle$ which complies with [7].

Modulation	AltBOC(15,10)
Bandwidth	$BW = 80$ MHz
Correlators' Setup	Optimal [31]
Early/Late Spacing	$\Delta\tau = T_c/18$
DLL Discriminator	Power
PLL Discriminator	Atan2
DLL Filter	3. order, 10 Hz, $D_\tau = 1$
PLL Filter	3. order, 20 Hz, $D_\varphi = 1$
$SNR = \alpha_0^2/(2N_0)$	20 dB
DLL Input Signal	Step: $0 \to 0.02T_c$
PLL Input Signal	Step: $0 \to \pi/3$
Carrier Phase Noise	$f_0 = 1$ Hz, $\mathcal{L}(f_0) = -100$ dBc/Hz
	$f_1 = 100$ Hz, $\mathcal{L}(f_1) = -120$ dBc/Hz

Tab. 1. Simulation setup.

The variance of the DLL equivalent loop noise exhibits multiple local minima, whereas the variance of the PLL equivalent loop variance is almost constant over the range of the interest. It corresponds to the shape of either discriminator characteristics.

The peaks of the alternating DLL multipath characteristics decline from its first maximum similarly as in [30]. The next two following subfigures depicting transient responses on the step functions document that both feed-back systems react relatively promptly. Be the sampling period of the simulation 1 ms, the DLL would get into the steady state within 0.3 s and the PLL within 0.7 s. The characteristics of mean square error depending on SNR were obtained as the steady-state values of the characteristics depicting the mean square error in time.

8. Conclusions

In this paper, we established a universal framework for description of GNSS modulations as special cases of the linear multi-dimensional modulation (LMDM). Namely, we introduced how BPSK(γ), BOC(β,γ), AltBOC(15,10) modulations can be represented in that manner. We extended the approach for IQ representation of the modulation, including CBOC modulation. A discussion on representation of TMBOC signals was delivered.

Based on the general description of the signals, basic semi-analytic model for simulations with correlation between the received signal and replicas of its modulation impulses has been developed. The model can represent an arbitrary number of correlations for various time shifts of the replicated modulation impulses. To represent more realistic scenarios, an extended model accounting for slowly fading multipath, finite bandwidth, phase noise, feed-back delay, and combination of these has been developed.

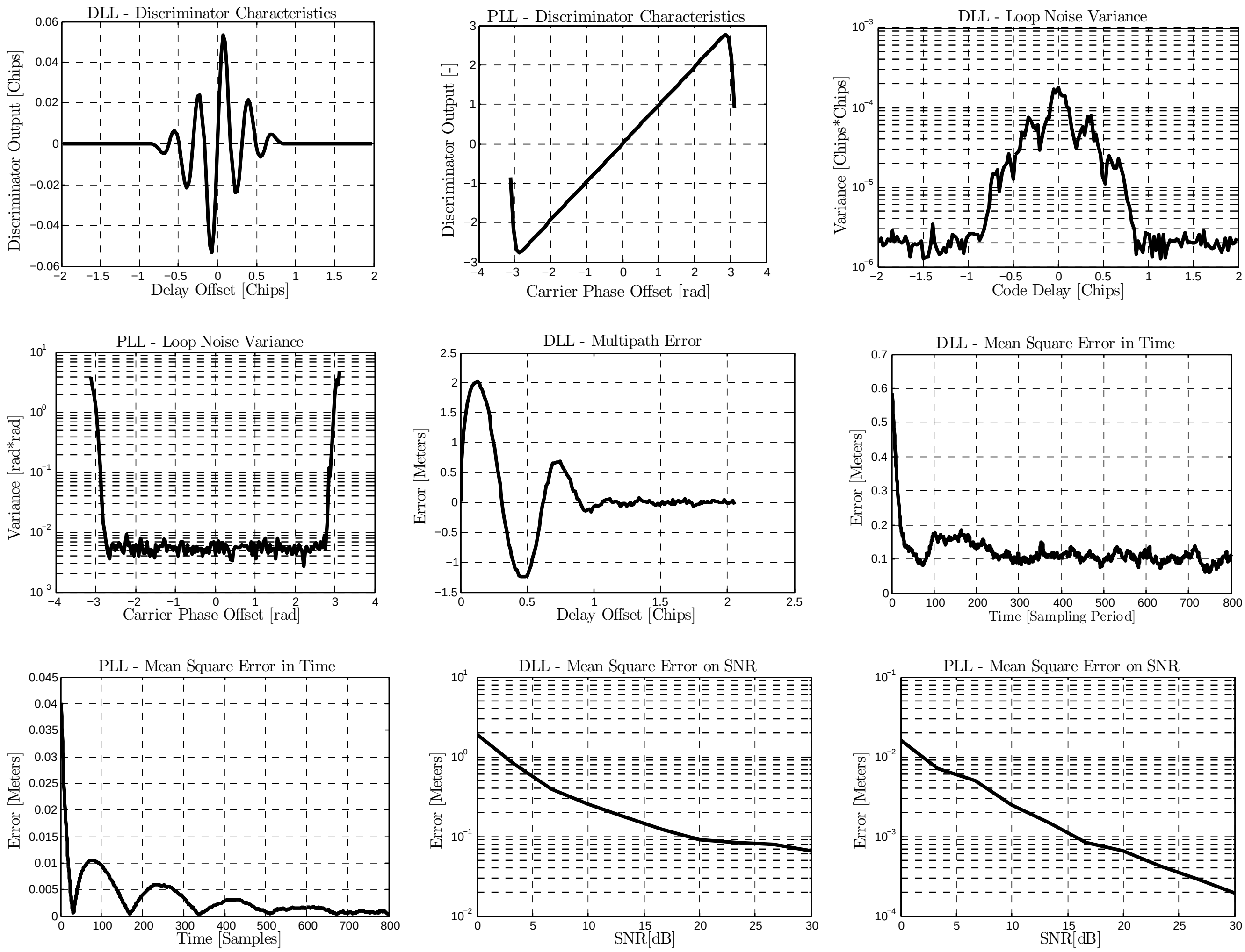

Fig. 10. Simulation results of the setup in Tab. 1. The multipath error is evaluated for the difference of carrier phase offsets $\varphi_1 - \varphi_0 = \pi$ and ratio of amplitudes $\alpha_0/\alpha_1 = 2$. The time axes of the mean square error figures are expressed in samples of the post-correlator processing.

The fact that the models need not be applied only to the tracking loops was discussed. We proposed it for simulations of complex systems including PVT estimation, vector tracking, direct positioning, multipath mitigation techniques, or simply elsewhere where the high-rate correlation in the above stated form appears.

Finally, we introduced a Matlab-based simulator with the extended model as a basic building block and demonstrated several characteristics of optimal AltBOC(15,10) processing by the code and carrier tracking loops.

Acknowledgements

SafeLOC is a project that is supported by public funds under Contract No. 20110198 with the Technology Agency of the Czech Republic in the program to support research and development ALFA.

References

[1] JERUCHIM, M. C., BALABAN, P., SHANMUGAN, K. S. *Simulation of Communication Systems: Modeling, Methodology and Techniques.* 2nd ed. New York (USA): Kluwer Academic/Plenum Publishers, 2000.

[2] TRANTER, W., SHANMUGAN, K., RAPPAPORT, T., KOSBAR, K. *Principles of Communication Systems Simulation with Wireless Applications.* Upper Saddle River (NJ, USA): Prentice Hall, 2003.

[3] GOLSHAN, A. R. Post correlator modeling for fast simulation and joint performance analysis of GNSS code and carrier tracking loops. In *Proceedings of the ION 2006 National Technical Meeting of the Institute of Navigation.* Montery (CA, USA), 2006, p. 312 - 318.

[4] SILVA, J. S., SILVA, P. F., FERNANDEZ, A., DIEZ, J., LORGA, J. F. M. Factored correlator model: A solution for fast, flexible, and realistic GNSS receiver simulations. In *Proceedings of the 20th International Technical Meeting of the Satellite Division of The Institute of Navigation (ION GNSS 2007).* Fort Worth (TX, USA), 2007, p. 2676 - 2686.

[5] BORIO, D., ANANTHARAMU, P. B., LACHAPELLE, G. Semi-analytic simulations: An extension to unambiguous BOC tracking. In *Proceedings of ION ITM 2010: International Technical Meeting of the Institute of Navigation.* San Diego (CA, USA), 2010, p. 1 - 14.

[6] BORIO, D., ANANTHARAMU, P. B., LACHAPELLE, G. SATL-Sim: A semi-analytic framework for fast GNSS tracking loop simulations. *GPS Solutions*, 2011, vol. 14, no. 4, p. 427 - 431.

[7] KAPLAN, E. D., HEGARTY, C. J. *Understanding GPS: Principles and Applications.* 2nd ed. Norwood (USA): Artech House, 2006.

[8] VAN NEE, R. D. J., SIEREVELD, J., FENTON, P. C., TOWNSEND, B. R. The multipath estimating delay lock loop: Approaching theoretical accuracy limits. In *Proceedings of the IEEE Position Location and Navigation Symposium.* Las Vegas (NV, USA), 1994, p. 246 - 251.

[9] DIERENDONCK, A. J., FENTON, P., FORD, T. Theory and performance of narrow correlator spacing in GPS receiver. *Navigation: Journal of the Institute of Navigation*, 1992, vol. 39, no. 3, p. 265 - 284.

[10] JONES, J., FENTON, P. C., SMITH, B. *Theory and performance of the pulse aperture correlator (NovAtel technical report).* 13 pages. [Online] Cited 2011-10-11. Available at: http://webone.novatel.ca/assets/Documents/Papers/PAC.pdf.

[11] LENTMAIER, M., KRACH, B., ROBERTSON, P. Bayesian time delay estimation of GNSS signals in dynamic multipath environments. *International Journal of Navigation and Observation*, 2008, 11 p.

[12] MISRA, P., ENGE, P. *Global Positioning System: Signals, Measurements, and Performance.* Lincoln (MA, USA): Ganga-Jamuna Press, 2001.

[13] COPPS, E. M., GEIER, G. J., FIDLER, W. C., GRUNDY, P. A. Optimal processing of GPS signals. *Navigation: Journal of the Institute of Navigation*, 1980, vol. 27, no. 3, p. 171 - 182.

[14] SPILKER, J. J. *Vector delay lock loop processing of radiolocation transmitter signals (US Patent 5398034).* [Online] Cited 2011-10-11. Available at: http://www.freepatentsonline.com/5398034.html.

[15] SPILKER, J. J. Fundamentals of signal tracking theory. *Global Positioning System: Theory and Applications*, Washington DC (USA): American Institute of Aeronautics and Astronautics, Inc., 1996, p. 245 - 327.

[16] PETOVELLO, M. G., LACHAPELLE, G. GNSS solutions: What are vector tracking loops and what are their benefits and drawbacks. *Inside GNSS*, 2009, vol. 4, no. 3, p. 16 - 21. [Online] Available at: http://insidegnss.com/node/1458.

[17] PANY, T., KANIUTH, R., EISSFELLER, B. Deep integration of navigation solution and signal processing. In *Proceedings of the 18th International Technical Meeting of the Satellite Division of The Institute of Navigation (ION GNSS 2005).* Long Beach (CA, USA), 2005, p. 1095 - 1102.

[18] PANY, T., EISSFELLER, B. Use of vector delay lock loop receiver for GNSS signal power analysis in bad signal conditions. In *Proceedings of IEEE/ION PLANS 2006*. San Diego (CA, USA), 2006, p. 893 - 903.

[19] CLOSAS, P., FERNANDEZ-PRADES, C., FERNANDEZ-RUBIO, J. A. Direct position estimation approach outperforms conventional two-step positioning. In *17th European Signal Processing Conference (EUSIPCO 2009)*. Glasgow (Scotland), 2009, p. 1958 - 1962.

[20] CLOSAS, P., FERNANDEZ-PRADES, C., FERNANDEZ-RUBIO, J. A. Maximum likelihood estimation of position in GNSS. *IEEE Signal Processing Letters*, 2007, vol. 14, no. 5, p. 359 - 362.

[21] The Witch Navigator Team. *GNSS Tracker*, Version 1.0. [Online] Cited 2011-10-26. Available at: http://witchnav.cz/lib/exe/fetch.php?media=people:gnss_tracker.tar.gz.

[22] PROAKIS, J. *Digital Communications.* 4th ed. New York (USA): McGraw-Hill, 2000.

[23] BETZ, J. W. Binary offset carrier modulations for radionavigation. *Navigation: Journal of the Institute of Navigation*, 2001 - 2002, vol. 48, no. 4, p. 227 - 245.

[24] European Union. *European GNSS (Galileo) Open Service - Signal In Space Interface Control Document (ICD Document).* Issue 1.1. [Online] Cited 2011-10-11. Available at: http://ec.europa.eu/enterprise/policies/satnav/galileo/open-service/index_en.htm.

[25] KACMARIK, P., KOVAR, P., VEJRAZKA, F. Galileo Alt-BOC E5 signal characteristics for optimal tracking algorithms. In *NAV08/ILA37 The Navigation Conference & Exhibition*. London (UK), 2009, p. 1 - 9.

[26] MEYR, H., ASCHEID, G. *Synchronization in Digital Communications, Volume I: Phase-, Frequency-Locked Loops and Amplitude Control.*. New York (USA): Wiley, 1990.

[27] MEYR, H., MOENECLAYE, M., FETCHEL, S. A. *Digital Communication Receivers. Synchronization, Channel Estimation and Signal Processing.* New York (USA): Wiley, 1998.

[28] KAY, S. M. *Fundamentals of Statistical Signal Processing: Estimation Theory.* New Jersey (USA): Prentice-Hall, 1993.

[29] JAKUBOV, O. *Assessment of Signal Tracking Algorithms Performance in GNSS.* Master's thesis. Prague (Czech Republic): Czech Technical University, 2010.

[30] SLEEWAEGEN, J. M., WILDE, W. D., HOLLREISER, M. *Galileo AltBOC Receiver (Septentrio, Technical Document).* [Online] Cited: 2011-10-11. Available at: http://www.septentrio.com/content/galileoaltboc-receiver.

[31] KOVAR, P., KACMARIK, P., VEJRAZKA, F. High performance Galileo E5 correlator design. In *Proceedings of 13th IAIN World Congress*. Stockholm (Sweden), 2009, p. 1 - 8.

About Authors...

Ondrej JAKUBOV was born in Liberec, Czech republic. He received his MSc in electrical engineering from the CTU in Prague in 2010. He is a postgraduate student at the same university at the Department of Radio Engineering. His research interests include GNSS signal processing algorithms and receiver architectures. His research focuses on advanced positioning and tracking methods. He is an active member of the team developing multi-system, multi-frequency, and multi-antenna GNSS receiver, named the Witch Navigator.

Petr KACMARIK was born in 1978. He received his MSc degree from the CTU in Prague in 2002. During his postgraduate studies (2002 - 2006) he was engaged in the investigation of satellite navigation receiver techniques in hard conditions and wrote his PhD thesis with its main topic on GNSS signal tracking using DLL/PLL with applicability to week signal environment. He defended the thesis in 2009. Since 2006 he works as an Assistant Professor at the Faculty of Electrical Engineering of the CTU in Prague. His main professional interests are satellite navigation, digital signal processing, implementations and simulations of signal processing algorithms.

Pavel KOVAR was born in Uherske Hradiste in 1970. He received his MSc and PhD degrees from CTU in Prague in 1994 and 1998, respectively. Since 1997 to 2000 he worked in Mesit Instruments as a designer of avionics instruments. Since 2000 he is with the Faculty of Electrical Engineering of the CTU in Prague as an Assistant Professor and since 2007 as an Associate Proffesor (Doc.). His interests are receiver architectures, satellite navigation, digital communications and signal processing.

Frantisek VEJRAZKA was born in 1942. He received his MSc degree from the CTU in Prague in 1965. He served as an Assistant Professor (1970) and Associate Professor (1981) at the Department of Radio Engineering. He is a full professor of radio navigation, radio communications, and signals and systems theory since 1996. He was appointed the Head of the Department of Radio Engineering (1994 – 2006), vice-dean of the Faculty (2000 – 2001) and vice-rector of the CTU in Prague (2001 – 2010). His main (professional) interest is in radio satellite navigation where he participated on the design of the first Czech GPS receiver (1990) for the Mesit Instruments. He was responsible for the development of Galileo E5 receiver for Korean ETRI during 2008 and E1 and E5a receiver in 2009. Prof. Vejrazka has published 11 textbooks, more than 200 conference papers and many technical reports. He is the former president of the Czech Institute of Navigation, Fellow of the Royal Institute of Navigation in London, member of the Institute of Navigation (USA), vice-president of IAIN, vice-chairman of CGIC/IISC, member of IEEE, member of Editorial Board of GPS World, Editorial Board of InsideGNSS, etc.